Conserved Induction of Distinct Antiviral Signalling Kinetics by Primate Interferon Lambda 4 Proteins

Cuncai Guo[1†], Dorothee Reuss[1†], Jonathon D. Coey[2], Swathi Sukumar[3], Benjamin Lang[4], John McLauchlan[5], Steeve Boulant[1,6,7], Megan L. Stanifer[7,8*] and Connor G. G. Bamford[2*]

[1] Department of Infectious Diseases, Virology, University Hospital Heidelberg, Heidelberg, Germany, [2] Wellcome-Wolfson Institute for Experimental Medicine, Queen's University Belfast, Belfast, United Kingdom, [3] Institute of Virology, University of Münster, Münster, Germany, [4] Exzellenzcluster Science of Intelligence, Technische Universität Berlin, Berlin, Germany, [5] Medical Research Council University of Glasgow Centre for Virus Research, University of Glasgow, Glasgow, United Kingdom, [6] Research Group "Cellular Polarity and Viral Infection", German Cancer Research Center (DKFZ), Heidelberg, Germany, [7] Department of Molecular Genetics and Microbiology, College of Medicine, University of Florida, Gainesville, FL, United States, [8] Department of Infectious Diseases, Molecular Virology, University Hospital Heidelberg, Heidelberg, Germany

Interferon lambdas (IFNλ) (also known as type III IFNs) are critical cytokines that combat infection predominantly at barrier tissues, such as the lung, liver, and gastrointestinal tract. Humans have four IFNλs (1–4), where IFNλ1–3 show ~80%–95% homology, and IFNλ4 is the most divergent displaying only ~30% sequence identity. Variants in IFNλ4 in humans are associated with the outcome of infection, such as with hepatitis C virus. However, how IFNλ4 variants impact cytokine signalling in other tissues and how well this is conserved is largely unknown. In this study, we address whether differences in antiviral signalling exist between IFNλ4 variants in human hepatocyte and intestinal cells, comparing them to IFNλ3. We demonstrate that compared to IFNλ3, wild-type human IFNλ4 induces a signalling response with distinct magnitudes and kinetics, which is modified by naturally occurring variants P70S and K154E in both cell types. IFNλ4's distinct antiviral response was more rapid yet transient compared to IFNλ1 and 3. Additionally, divergent antiviral kinetics were also observed using non-human primate IFNλs and cell lines. Furthermore, an IFNλ4-like receptor-interacting interface failed to alter IFNλ1's kinetics. Together, our data provide further evidence that major functional differences exist within the IFNλ gene family. These results highlight the possible tissue specialisation of IFNλs and encourage further investigation of the divergent, non-redundant activities of IFNλ4 and other IFNλs.

Keywords: interferon, lambda, signalling, antiviral, *IFNL4*, kinetics

INTRODUCTION

Viral infections of mucosal surfaces like the lung, gut, and liver [such as influenza, rotavirus and hepatitis C virus (HCV)] remain major drivers of global morbidity and mortality in the human population (1). The host innate immune response is a critical determinant of the outcome of infection and as such, its stimulation can influence clinical outcomes (2). Following sensing of viral infection, several antiviral and immunoregulatory factors like cytokines are induced that act to limit viral replication and promote clearance and long-term immunity (3). Interferons (IFNs) are one important group of such cytokines with potent antiviral activity (4). There exist three recognised families of IFNs: the type I IFNs (alpha 1-13, beta, epsilon, kappa, and omega in humans), type II IFNs (gamma), and type III IFNs [lambdas (λ) 1–4] (5). Types I and III IFNs are rapidly induced and secreted following sensing of infection in most nucleated cells. These secreted IFNs then act in turn on the infected cell and on neighbouring uninfected cells to induce the production of hundreds of interferon stimulated genes (ISGs) *via* activation of the Janus kinase–signal transducer and activator of transcription (JAK-STAT) pathway. Although they share similar downstream signalling pathways and lead to the activation of similar ISGs, type I and III IFNs utilise distinct cell surface receptor complexes (6). Type I IFNs use the ubiquitously expressed IFNAR1 and IFNAR2 heterodimeric complex, whilst type III IFNs use the IFNλR1 and IL10R2 heterodimeric complex. Although also found on some immune cell types (7), IFNλR1 is predominantly expressed on epithelial cells at the so-called barrier tissues (8), including the respiratory and gastrointestinal tracts, and hepatocytes in the liver of humans (9), which provides type III IFNs distinct traits specialised in the protection of mucosal surfaces compared to type I IFNs (10–12).

Although they share a receptor complex, there is emerging evidence that not all type III IFNs have redundant features (13). The human IFNλs, namely, IFNλ1, IFNλ2, and IFNλ3, all share >80% homology, yet compared to IFNλ4, they exhibit only ~30% homology (6, 9, 13). Whilst all type III IFNs are more recently discovered in comparison to type I IFNs (4, 6, 9), IFNλ4 was the latest addition to the family being only identified in 2013 (13). The outcome of HCV infection is associated with genetic variation in the human *IFNL* locus [e.g., "*IL28B*" single nucleotide polymorphisms (SNPs)], likely mediated by variants within *IFNL4* (14). IFNλ4, like other IFNλs, has potent antiviral activity (15). These same genetic variants are also associated with extra-hepatic infections, such as enteroviral infection in the respiratory tract (16). There are two common loss-of-function SNPs in human *IFNL4*, encoding a frameshift (rs12979860), and a non-synonymous variant P70S (rs117648444, which encodes a proline to serine mutation at position 70), respectively (13, 14). Whilst the frameshift ablates IFNλ4 production, P70S reduces the potency of ISG induction by IFNλ4 (14, 17, 18). Interestingly, it is these hypo- or inactive alleles that are associated with protection from chronic HCV infection in humans (13, 14).

Further investigation into the functional diversity of IFNλ4 identified two rare variants that affect IFNλ4 activity, including an additional hypoac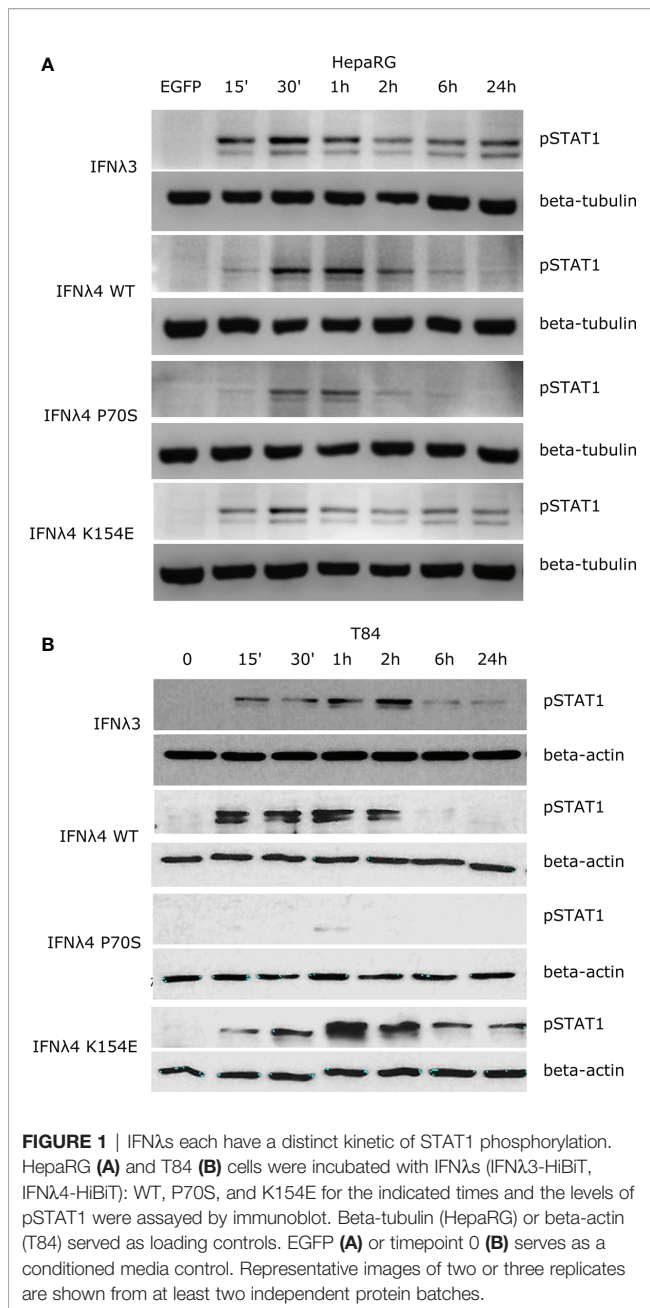tive variant L79F (leucine to phenylalanine at position 79) and K154E (lysine to glutamic acid at position 154), which dramatically enhances IFNλ4 antiviral activity by increasing its secretion and potency (17). Intriguingly, although K154 is nearly ubiquitous in the human population, E154 is the ancestral amino acid at this position in non-human primates and other mammals. E154 was found in a small number of extant humans. Accordingly, chimpanzee and rhesus macaque IFNλ4 have enhanced antiviral activity relative to wild-type human IFNλ4, which can be reversed by an E154K mutation. Together, the evolutionary data suggest a step-wise attenuation of IFNλ4 activity (E154K > P70S > TT frameshift) unique to modern humans (13), which is consistent with the non-redundancy of IFNλ4 compared to other IFNλs. However, which precise unique biological feature(s) of IFNλ4 that are non-redundant (and thus have been acted upon by evolution) are poorly understood and only beginning to be unravelled (14, 19, 20).

Following on from our previous work (11, 17), we wished to determine how the antiviral activity of IFNλ4 and its variants and homologues changed in a time-dependent manner, compared to other IFNλs. To test this hypothesis, we characterised the kinetics of signalling and antiviral activity of a panel of IFNλ4 variants in human hepatocyte and human intestinal epithelial cells compared to IFNλ3. Together, our work demonstrates the unique kinetics of IFNλ4 activity compared to other IFNλs, which is conserved within and between species. Further work on the intrinsic differences between IFNλ4 and other IFNs is warranted.

RESULTS

IFNλ Variants Display Unique STAT1 Phosphorylation Kinetics

Binding of IFNλs to their receptor complex leads to activation of downstream signalling cascades that ultimately lead to the establishment of an antiviral state (6). The JAK/STAT pathway is one of the most critical and well-characterised pathways activated following IFNλ binding. An emerging view is that the kinetics of such a downstream response is a crucial determinant of the antiviral potential of IFNλs (11, 20). To probe the temporal basis of IFNλ signalling in greater detail, we first measured phosphorylation of STAT1 over time at Y701 (**Figure 1**). Human hepatocyte HepaRG monolayers were incubated with conditioned media estimated to contain equivalent amounts of IFNλs (IFNλ3, IFNλ4 WT, P70S, L79F, and K154E) for 15, 30, 60, 120, and 360 min, and 24 h. Following stimulation, protein lysates were harvested, and STAT1 phosphorylation was assayed by immunoblot analysis (**Figure 1A**). Conditioned media generated following transfection of an enhanced green fluorescent protein (EGFP)-expressing plasmid served as a negative control. Results showed that IFNλ3 and a number of IFNλ4 variants induced detectable levels of pSTAT1 (**Figure 1A**, quantified in **Supplementary Figure 1A**). L79F gave extremely low levels of pSTAT1 (data not shown), which likely correlates with its very limited activity as described previously (17). Interestingly, IFNλ3 and IFNλ4

FIGURE 1 | IFNλs each have a distinct kinetic of STAT1 phosphorylation. HepaRG **(A)** and T84 **(B)** cells were incubated with IFNλs (IFNλ3-HiBiT, IFNλ4-HiBiT): WT, P70S, and K154E for the indicated times and the levels of pSTAT1 were assayed by immunoblot. Beta-tubulin (HepaRG) or beta-actin (T84) served as loading controls. EGFP **(A)** or timepoint 0 **(B)** serves as a conditioned media control. Representative images of two or three replicates are shown from at least two independent protein batches.

variants induced distinct kinetics of pSTAT1 activation (**Figure 1A** and **Supplementary Figure 1A**). Whilst all IFNλs peaked around similar times (30 min to 1 h), IFNλ4 WT and P70S showed clear transient activation, whilst IFNλ3 and K154E displayed persistent activation of pSTAT1. Importantly, levels of pSTAT1 correlated with previously measured antiviral potential for three IFNλ4 variants K154E > WT > P70S (17). As IFNλs can also signal in other tissues apart from the human liver (8, 21), and there is an emerging role for IFNλ4 in extra-hepatic environments, we assayed whether human colon carcinoma cells (T84) were capable of inducing pSTAT1 in response to IFNλ4 and its variants. Intestinal T84 cells were treated and incubated with conditioned media containing equivalent

amounts of IFNλs (IFNλ3, IFNλ4 WT, P70S, and K154E), and their induction of pSTAT1 was assayed over time by immunoblot analysis (**Figure 1B** and **Supplementary Figure 1B**). We observed similar trends as to HepaRG, although differences in amplitude of pSTAT1 induction were noted, especially for IFNλ4 K154E in T84 cells. Together, these results show that both hepatic and intestinal cell lines can respond to both IFNλ3 and IFNλ4 and display variant-specific inductions of the JAK/STAT pathway.

IFNλ Variants Display Different Levels of ISG Induction

Phosphorylation of STAT1 following receptor complex engagement by IFNλs results in STAT1/2 dimer formation and translocation to the nucleus to induce ISG transcription, which ultimately leads to the production of antiviral proteins and the establishment of an antiviral state (6). Our previous work showed that IFNλ variants induced different levels of ISG expression when measured at 24 h (17). To ascertain whether this ISG expression varied at earlier times after incubation in concert with the kinetics of pSTAT1 activation, we measured the relative induction of a panel of core ISGs (*IFIT1*, *MX1*, *ISG15*, and *RSAD2/VIPERIN*) compared to EGFP-treated conditioned media in HepaRG cells (**Figures 2A–D**) and T84 cells (**Figures 2E–H**). Compared to EGFP-conditioned media stimulated cells, all IFNλs induced measurable increases in ISG mRNA in HepaRG cells but with discernible differences in magnitude. T84 cells also showed ISG induction for four of the supernatants tested (**Figures 2E–H**). Additionally, looking at relative fold change, T84 cells gave a lower induction of all ISGs as compared to HepaRG cells (**Figure 2**). The magnitudes of ISG induction for both cell lines mirrored the pSTAT1 induction that was observed in **Figure 1** (IFNλ3/K154E > WT > P70S > L79F). IFNλ4 K154E induced a similar pattern of ISG induction as IFNλ3 in both cell lines. Interestingly the kinetics of ISG induction was distinct to each cell line. In HepaRG cells, all IFNλs induced an early peak induction of ISGs, which subsequently declined over time. Moreover, IFNλ4 K154E demonstrated a slightly faster induction and peaked by 2 h whilst all other IFNλs tested peaked at 6 h. By contrast, IFNλ3 and the IFNλ4 K154E showed no or little decline in ISG induction after induction at either 2 or 6 h in T84 cells (**Figures 2E–H**). Additionally, T84 cells yielded low to almost undetectable induction of ISGs following IFNλ4 WT and P70S treatment. Together, these results show that K154E provides similar stimulatory activity to IFNλ3 and that this is far greater than for either IFNλ4 WT or P70S, which are the most common IFNλ4 variants in the human population.

IFNλ Variants Have Distinct Antiviral Activity in Intestinal Cells

Induction of an antiviral state is the major downstream consequence of IFN signalling. To determine how STAT1 phosphorylation and ISG expression correlate with antiviral activity, we infected the hepatic and intestinal cell models with two different viruses, EMCV and VSV. Both EMCV and VSV are
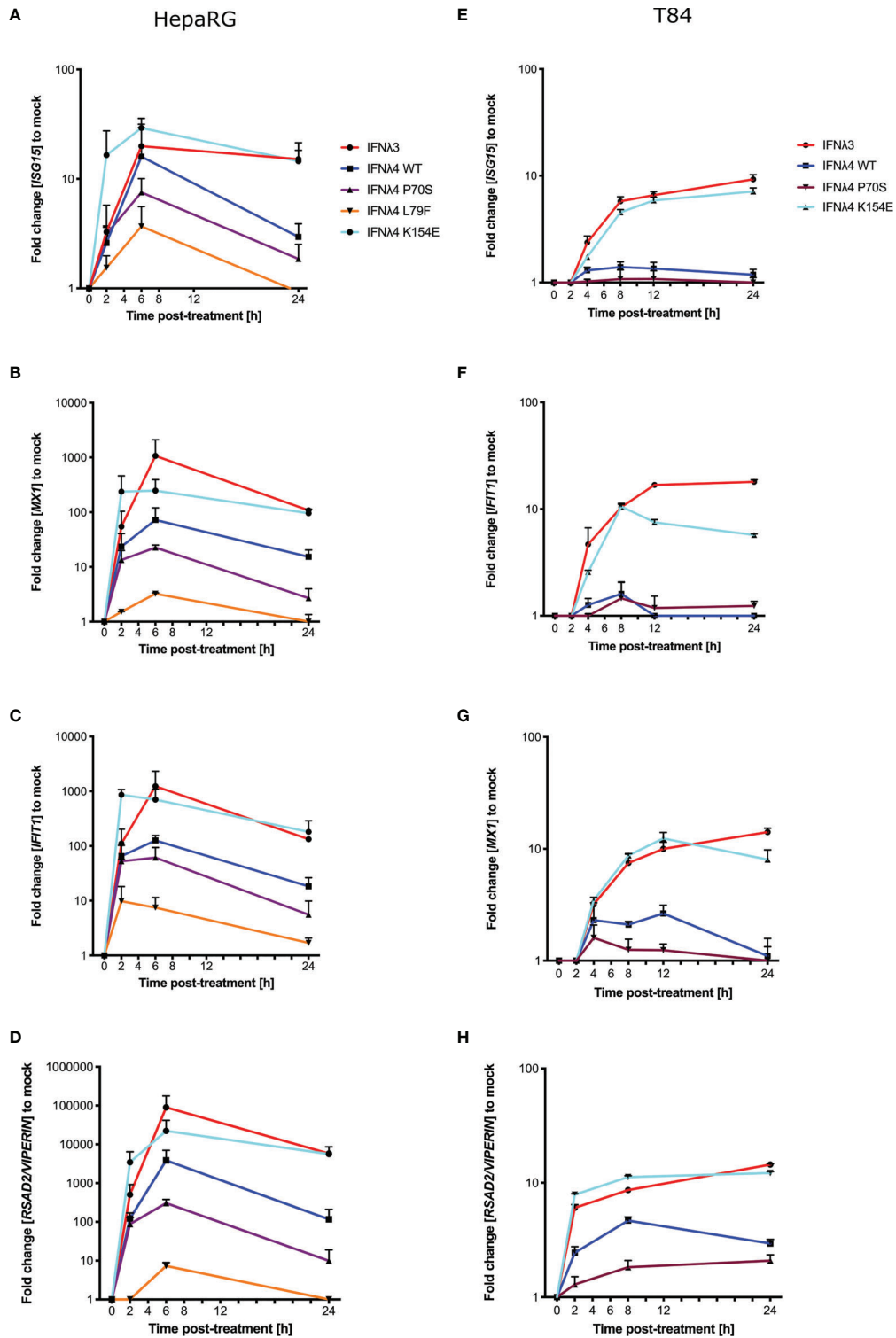
FIGURE 2 | IFNλ variants induce unique magnitudes of ISG mRNA. HepaRG **(A–D)** and T84 **(E–H)** cells were incubated with IFNλs [IFNλ3-HiBiT (red); IFNλ4-HiBiT: WT (blue), P70S (purple), L79F (yellow), and K154E (cyan)] for indicated times. At the respective time, total RNA was isolated, and qRT-PCR was performed for ISGs: *IFIT1* **(A, E)**, *ISG15* **(B, F)**, *MX1* **(C, G)**, and *RSAD2/VIPERIN* **(D, H)**. Mock control cells were treated with conditioned media from EGFP-plasmid transfected HEK-293T cells, and all values were normalised against this value at each time. *GAPDH* (HepaRG) or *HPRT1* (T84 cells) were used as housekeeping genes. L79F did not induce any detectable ISG induction in T84 cells. Error bars represent the mean ± SEM from two to three biological replicates from at least two independent protein batches.

highly cytopathic, replicate very fast, and are sensitive to IFN, which makes them suitable for assessing the kinetics of antiviral activity. EMCV infectivity and replication were assayed by determining the cytopathic effects of the virus, whilst a VSV encoding luciferase (VSV-luc) was deployed and its infectivity was measured by luciferase assay. HepaRG and T84 cells were treated with increasing concentrations of EGFP or IFNλ3 or IFNλ4-containing supernatants at 24 h prior to virus infection. Following IFNλ pretreatment, cells were infected with EMCV or VSV [multiplicity of infection (MOI) of 0.3 and 1, respectively] in the continuous presence of IFNλs, and infection was assayed at 24 h post-infection for EMCV (**Figure 3A**) and 8 h post-infection for VSV (**Figures 3B, C**). Different assay times for VSV versus EMCV were due to differences in replication kinetics and cytopathic effects of either virus. Consistent with our previous work (17, 21), results show that VSV infection was inhibited by all IFNs in both cell lines (**Figures 3B, C**). IFNλ3 was the most potent IFN, as it reduced VSV infection with 10% of the maximum concentration in both HepRG and T84 cells. IFNλ4 WT and K154E showed similar antiviral activity; however, a much higher concentration of these two IFNs was required to reach a similar potency as IFNλ3. Consistent with previous low pSTAT1 and ISG inductions, P70S was only able to slightly reduce virus infection even at the highest concentrations in both cell lines. T84 cells were poorly infected with EMCV and highly resistant to the cytopathic effects of the virus, and therefore, antiviral activity was not assayed in this cell line, but similar patterns of antiviral activity were seen for HepaRG cells infected with EMCV (**Figure 3A**).

IFNλ Variants Have Distinct Kinetics of Antiviral Activity

Having established antiviral assays in both liver- and intestinal-derived cell lines, we wished to determine whether IFNλ activity was time dependent and whether the continuous presence of IFNλs was required to maintain their antiviral activity. Therefore, we performed infections and antiviral assays over time, both in the continuous presence of IFNλs but also in cells that had been pretreated with IFNλs for varying lengths of time, yet the cytokines were then removed, monolayers washed, and fresh media provided ("non-washed" and "washed", respectively, **Figure 4A**) prior to infection. Initially, we conducted experiments in T84 cells that were infected with VSV following IFNλ pretreatment (**Figures 4B–E**). For clarity, it should be noted that the following data are presented differently than those in **Figure 3**. In agreement with the data presented in **Figure 3**, all IFNλs demonstrated antiviral activity with IFNλ3 and IFNλ4 P70S showing the greatest and least potency, respectively. The peak of IFNλ3 activity was delayed relative to all IFNλ4s. Moreover, we found that shorter incubation times with IFNλ3 followed by its removal before infection reduced its antiviral activity to a greater extent compared to the three IFNλ4 variants used in the experiment (compare early time points in **Figure 4B** with **Figures 4C–E**); comparison of activity between washed and unwashed was significant (t-test) at all time points for IFNλ3, whilst for IFNλ4s, it was only significant for the first or second

time points. In HepaRG cells infected with EMCV, we observed a similar pattern, i.e., removal of IFNλ3 after relatively short incubation (2 h) with cells gave a greater reduction in antiviral activity compared to the same timepoint for the IFNλ4 variants (**Figures 4F–I**); when compared with the difference between washed and unwashed for IFNλ4, that of IFNλ3 reached statistical significance (t-test). In addition, we observed that all IFNλs generally gave less antiviral activity after removal at the time of infection compared to activities in the continuous presence of the proteins. From these experiments, we suggest that IFNλ4 proteins may be more tightly bound to the heteromeric cell receptor as compared to IFNλ3. Alternatively, signalling with IFNλ4 is maintained for a longer period as compared to IFNλ3. To further assess the contribution of IFN-cell contact time compared to signalling time, we repeated the wash experiments in HepaRG cells with EMCV, but, on this occasion, cells were incubated with the IFNλs at 24 h prior to infection but then removed by washing at differing times before virus addition (**Supplementary Figure S2**). The results show a greater decline in antiviral activity (~15-fold) from 24 h incubation to 6 and 2 h incubation for IFNλ3 compared to IFNλ4 WT and IFNλ4 K154E, which showed reductions in activity by ~0.75-4 fold.

Divergent Kinetics Is Independent of Human IFNλ System

Our data suggest that in human cells, human IFNλ4 and its variants induce a distinct antiviral response compared with human IFNλ3. As previous work has demonstrated that IFNλ4 from different primate species have varying levels of antiviral activity (17, 22), we next explored whether the distinct signalling kinetics that we observed were also species specific. We first analysed the amino acid homology between IFNλ3, IFNλ4, IFNλR1, and IL10R2 in humans, chimpanzees, and rhesus macaques (**Figure 5A**). Results showed that although the various orthologues shared a high degree of homology (92-97%), there were differences that could affect activity given that even a single amino acid change can alter signalling as in IFNλ4 variants P70S and K154E. Given these genetic differences, we next tested the antiviral kinetics of non-human IFNλs. First, we treated human HepaRG cells with human and non-human IFNλs as described in **Supplementary Figure 2**, by treating cells for 2, 6, and 24 h, and then removing the cytokines prior to infection with EMCV at 24 h after initial stimulation (**Figure 5B**). For these experiments, we utilised non-human primate IFNλ3 or IFNλ4 proteins containing a C-terminal FLAG tag, which we characterised previously (17). In these experiments, we utilised IFNλ4 K154E as a model human IFNλ4, since it gave robust levels of detectable antiviral activity, with kinetics broadly similar to IFNλ4 WT. All IFNλs had antiviral activity against EMCV with chimpanzee IFNλ4 having greater activity than human and macaque IFNλ4 (**Figure 5C**), whilst human IFNλ3 had greater activity than macaque IFNλ3 (**Figure 5D**). Similar to human variants, the peak of IFNλ3 activity was delayed relative to all IFNλ4s. IFNλ3 washing experiments demonstrated that like human IFNλ4,
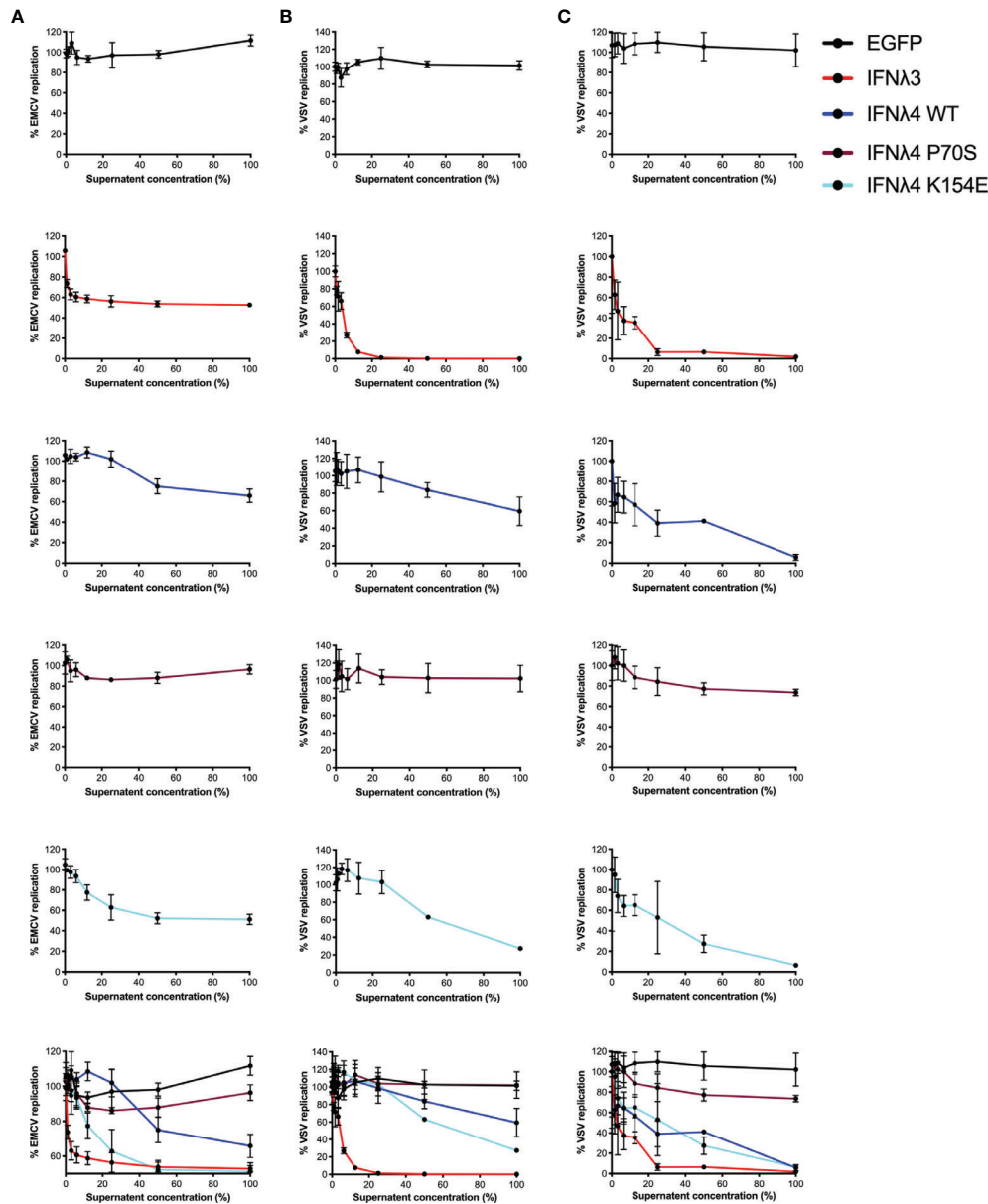
FIGURE 3 | Antiviral activity against EMCV or VSV of IFNλs on HepaRG and T84 cells. HepaRG **(A, B)** or T84 **(C)** cells were stimulated with different concentrations of supernatant containing the panel of IFNλs [IFNλ3-HiBiT (red); IFNλ4-HiBiT: WT (blue), P70S (purple), and K154E (cyan)] before being challenged with EMCV **(A)** or VSV **(B, C)** and antiviral activity calculated, shown here as percentage of viral replication at each dilution compared to mock (EGFP conditioned media treated) treated controls. Error bars represent the mean ± SEM from two to three biological replicates.

non-human primate IFNλ4 were more refractory to early removal than human or macaque IFNλ3 (**Figures 5C, D**). To determine if these characteristics also occurred in non-human cells, we repeated these experiments in the rhesus macaque respiratory epithelial cell line LLCMK2 (**Figures 5E, F**). Results showed that all IFNλ4s had similar kinetics of antiviral activity but different levels of potencies as found in HepaRG cells. Washing following immediate infection supported the initial washing experiments with IFNλ3 antiviral activity being more sensitive to early removal of cytokine (**Figures 5G, H**).

IFNλ1 With Receptor-Interacting Face Mutations Retain Parental Kinetics

Complex and dynamic interactions between cytokine ligands and their cognate receptors dictate the signalling output (23). To probe further the molecular genetic basis of IFNλ kinetics, we sought to mutate and disrupt the receptor binding faces of IFNλ, hypothesising that these residues were most likely to be responsible for IFN kinetics. IFNλ4 is highly divergent when compared with IFNλ1-3 with ~30% similarity detected,
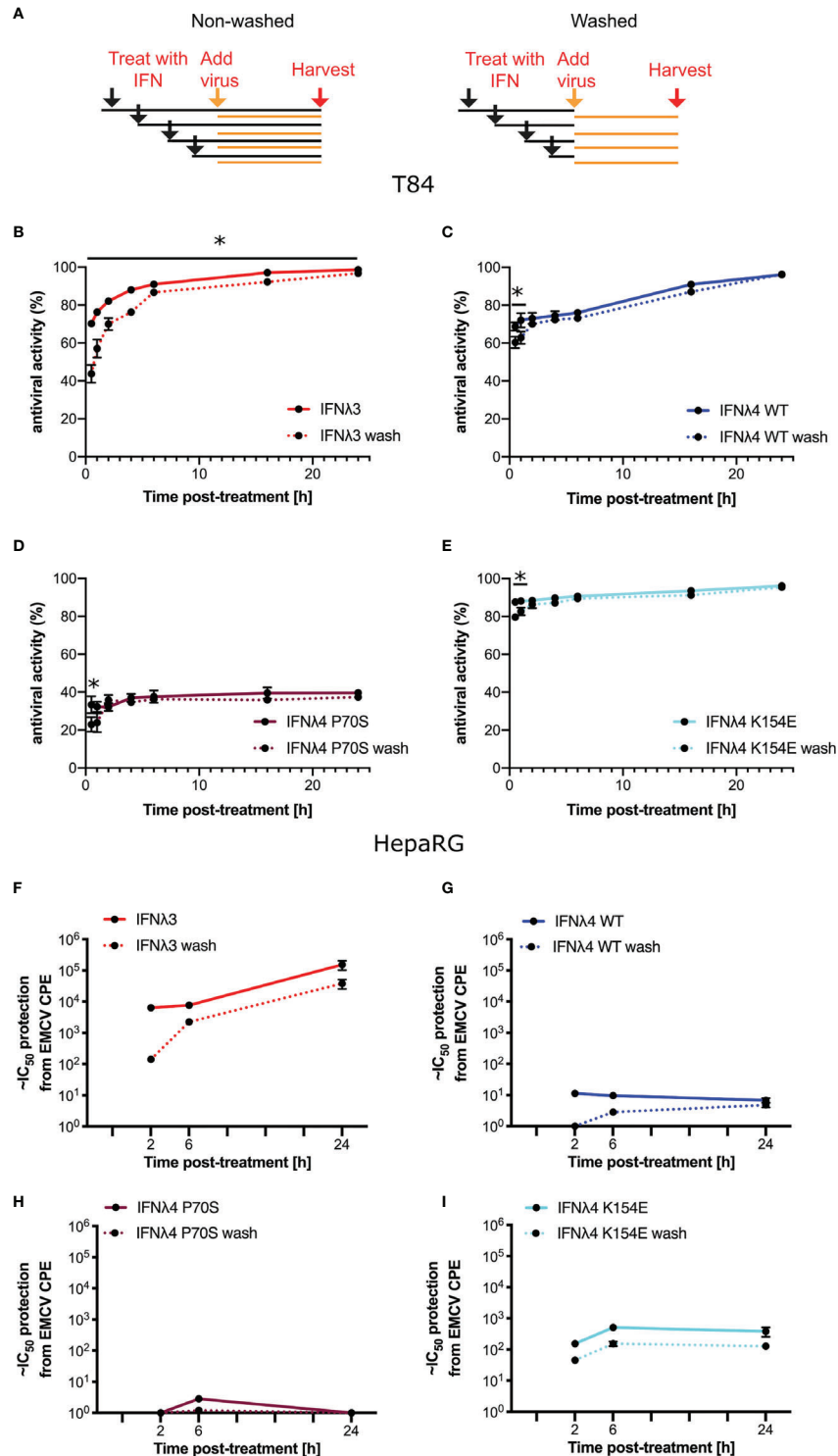
FIGURE 4 | Antiviral activity does not require continued presence of IFNλs. (A) Schematic description of the experiment to show how IFNλ was added and maintained or removed by washing. T84 (B–E) and HepaRG (F–I) were stimulated with IFNλs: IFNλ3-HiBiT (B, F), IFNλ4-HiBiT WT (C, G), P70S (D, H), and K154E (E, I) at indicated time prior to infection with EMCV (HepaRG) or VSV (T84). VSV-luc (B–E) was assayed 8 h post-infection by quantifying the luminescence (T84). EMCV infection (F–I) was assayed by analysis of its cytopathic effect 24 h postinfection of a series of twofold serial dilutions of supernatant. For washing experiments (dashed lines), IFNλs were removed and rinsed with PBS before being replaced with media containing virus. Error bars represent the mean ± SEM from two to four biological replicates from one (T84) or two (HepaRG) independent protein batches. Statistical significance is shown (*p≤0.05).
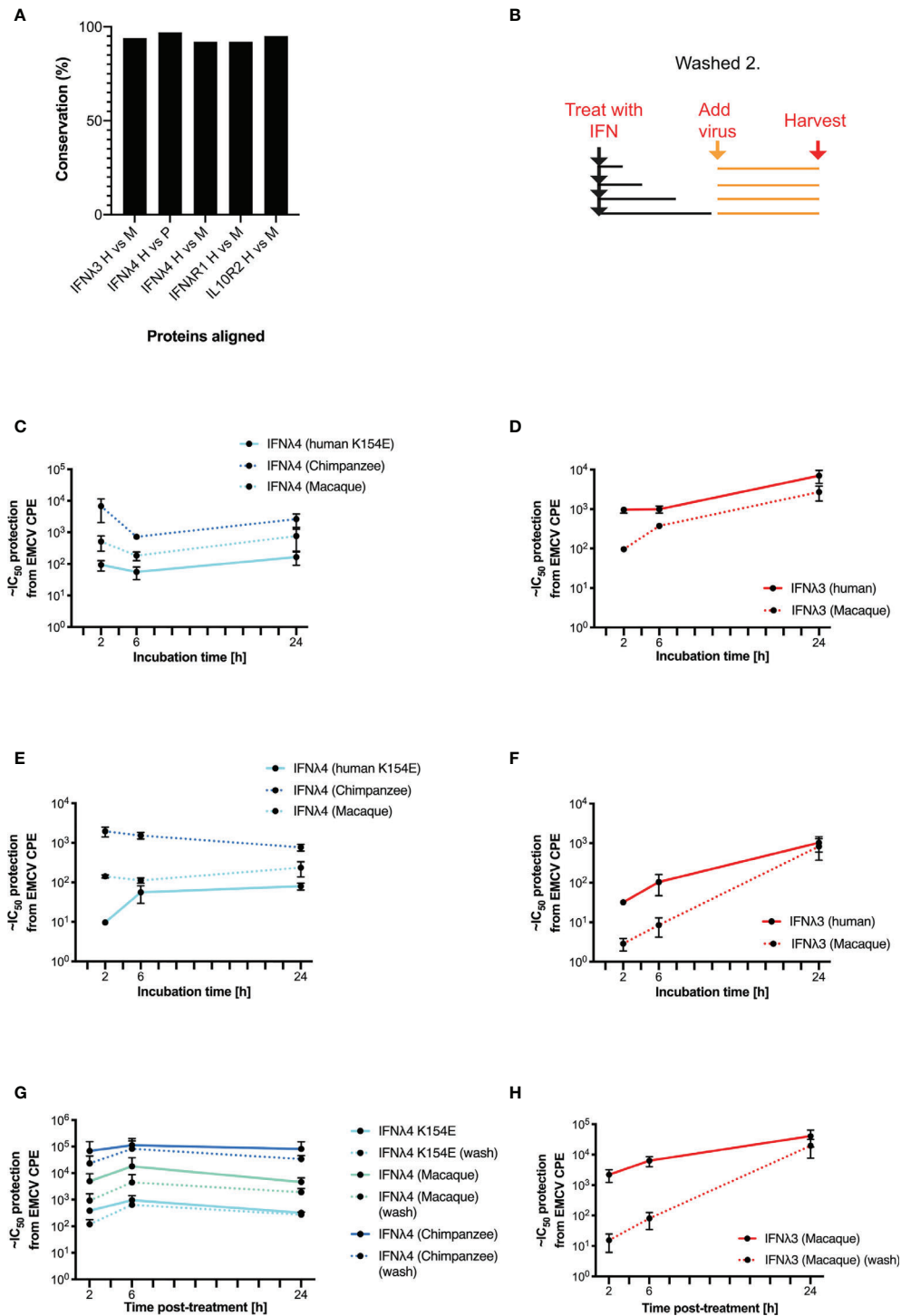
FIGURE 5 | Kinetics of antiviral activity of non-human primate IFNλs. The percentage identity of IFNλ pathway proteins (IFNλ3, IFNλ4, IFNλR1, and IL10R2) between humans, chimpanzees, and/or macaques was measured using BLAST **(A)**. A washing/incubation protocol was used **(B)** and HepaRG **(C, D, G, H)** or rhesus macaque LL-CMK2 **(E, F)** cells were pretreated with IFNλ4 **(C, E, G)** or IFNλ3 **(D, F, H)** for the indicated times prior to infection with EMCV. Times 24 (HepaRG) or 72 (LL-CMK2) hours postinfection antiviral activity was measured by CPE assay. Antiviral activity of IFNλs on HepaRG cells was measured using the alternative washing protocol **(G, H** outlined in **Figure 4)**. Results are shown as mean ± SD from four biological replicates. Data for panels **(A–F)** were obtained using independent protein batches as panels **(G, H)**.

suggesting that there are likely to be distinct molecular determinants of differential signalling contained within IFNλ4 compared to the other human IFNλs (13, 15). To begin to identify those determinants, we constructed chimeric IFNλs between IFNλ4 and human IFNλ1. IFNλ1 was chosen, as it is known to have similar kinetics to IFNλ3 (10) but, like IFNλ4, is N-linked glycosylated (6). Initially, comparison of differentially conserved amino acids in IFNλ4 (human and non-human primate) with IFNλ1-3 (human and macaque) identified a divergent receptor binding interface between these groups of IFNλs suggestive of distinct receptor interactions (**Figure 6A**). We focused on divergent, likely surface-exposed residues near

relevant helices (A, D, and F) and designed two chimeric IFNλs based on IFNλ1 containing candidate IFNλ4 residues from the IFNλR1-binding helix F (F) and the IL10R2-binding helices A and D (AD). An additional chimera with all three IFNλ4 binding helices was generated, termed ADF.

We first confirmed that IFNλ1 and its chimeras were produced and released into the supernatant using a split-luciferase assay; this showed that chimeras incorporating helices A and D yielded reduced production (**Figure 6B**). To test their antiviral activity, HepaRG cells were pretreated for 2, 6, or 24 h prior to EMCV infection with the WT IFNs and each of the indicated chimeras. Results showed that IFNλ1 had higher
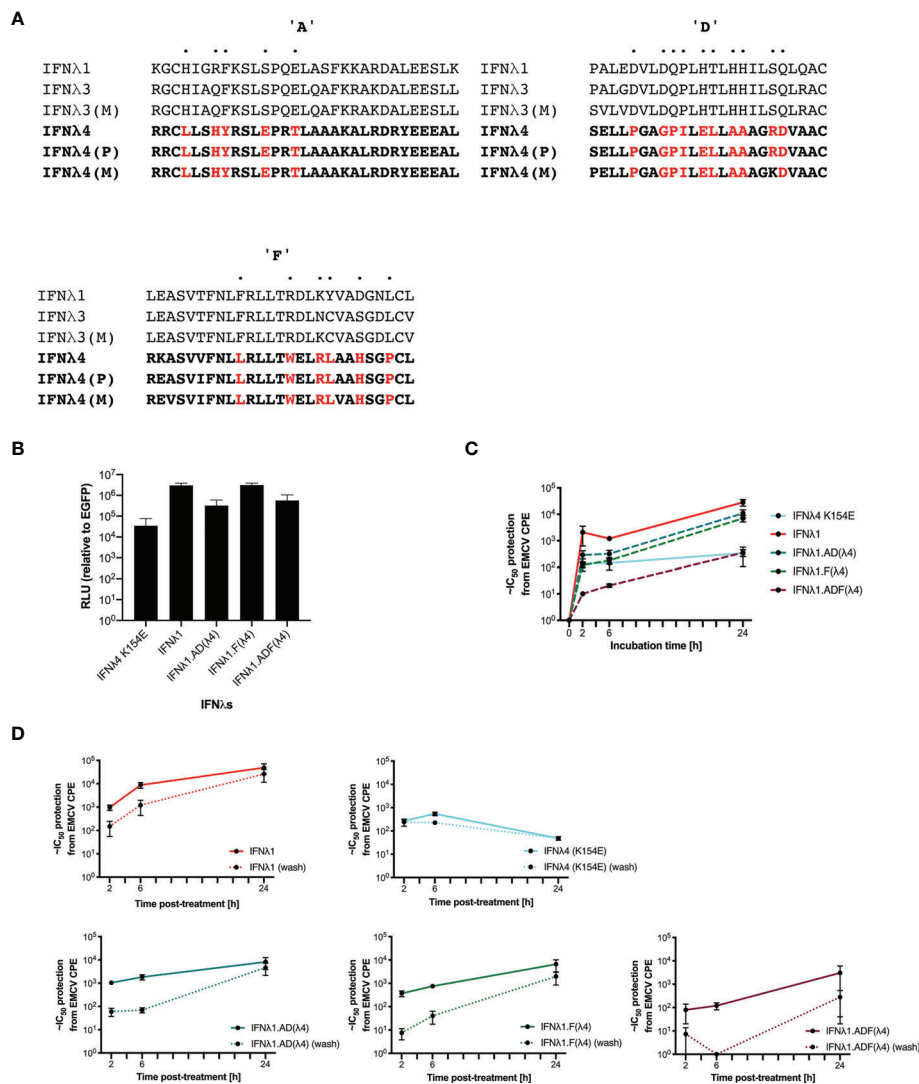

FIGURE 6 | IFNλ1 receptor-interacting interface mutants retain their kinetics. IFNλ1/4 chimeras were generated based on critical differences in helices **(A, D, F)** identified by alignment and comparative approaches. Specific positions in helices only were modified to those found in IFNλ4 (red) **(A)**. Relative levels of IFNλs in supernatant by HiBiT assay following transfection of expression plasmids into HEK-293T cells measured at 48 h after transfection **(B)**. Effect of incubation time (2, 6, or 24 h) **(C)** and washing (2, 6, or 24 h, washed as hashed lines) **(D)** of antiviral activity in HepaRG cells against EMCV was calculated as outlined previously. Hatched line indicates limit of detection of that experiment. Error bars represent the mean ± SEM from two to four biological replicates. Data for Panel **(C)** was generated using independent protein batches as Panel **(D)**.

antiviral activity than IFNλ4 yet similar to IFNλ3. Additionally, IFNλ1 with IFNλ4 substitutions had reduced antiviral activity (IFNλ1 > F > AD > ADF) (**Figures 6C, D**). To determine if the chimeras impacted IFN kinetics, HepaRG cells were pretreated for 2, 6, or 24 h prior to EMCV with the WT IFNs and each of the indicated chimeras. The IFNs were either left for the duration of the infection or removed at the time of infection, and infection was commenced either at time of cytokine removal or at 24 h after initial incubation. Importantly, IFNλ1 kinetics were similar to IFNλ3 in HepaRG cells, with increasing activity over time and a delayed peak relative to IFNλ4 (**Figures 6C, D** compared with **Figure 2F** and **Supplementary Figure 2**). IFNλ1/4 chimeras had similar kinetic profiles as IFNλ1. Results revealed that washing reduced the antiviral potency of all IFNs and IFNλ1, and all the chimeras were more greatly affected than IFNλ4. Taken with our antiviral activity results suggested that chimera F had reduced potency compared to IFNλ1, whilst the reduced activity of AD is likely due to reduced protein, and thus, the impact on ADF is due to reduced amount and potency (**Figure 6B**). However, despite alteration of the receptor interaction surfaces, the kinetics remain conserved similar to IFNλ1 (and IFNλ3), suggesting that these residues only modify the magnitude of the antiviral response and are not sufficient to alter the antiviral kinetics.

Altogether, our work described here demonstrates the distinct yet conserved antiviral kinetics of human and non-human primate IFNλ4 compared to other IFNλs.

DISCUSSION

Knowledge of the molecular signalling pathways stimulated by IFN binding is essential to understand immunity to infectious diseases and could help develop more effective interventions. The dynamics of antiviral signalling is emerging as a physiologically relevant and important topic, and several groups have shown that type III IFNs have distinct slower but sustained signalling kinetics compared to type I IFNs (10, 11, 21). Very few studies have addressed whether different members of the type III IFN family also have a similar kinetics for the activation of STAT1, induction of downstream ISGs, and antiviral activity (20). Through several lines of genetic evidence, it appears that human IFNλ4 has non-redundant functions relevant to immunity compared to other IFNλs, yet the determinants of this unique biology are poorly understood (13, 14). Additionally, there exist a number of naturally occurring functional variants of IFNλ4 that are known to impact potency (14, 17, 18). In this work, we addressed whether IFNλ4 WT and its variants (e.g., P70S and K154E) have altered antiviral kinetics, in comparison to IFNλ1 and IFNλ3. By comparing IFNλ4 signalling and antiviral activity in two cell lines from two distinct organs, we were able to identify conserved and variable features of IFNλ4 and IFNλ3 signalling that demonstrated distinct antiviral kinetics, consistent with recent studies (20). Critically, we also show that common (P70S) and rare (K154E) human variants predominantly impact the magnitude of IFN signalling but not the kinetics of that response, and these dynamics are largely conserved in non-human primate IFNλs and their cognate cell lines.

Comparison of IFN activity across variants is notoriously challenging given the need for input normalisation and relevant processing. To circumvent these issues, we produced IFNλ in human cells (HEK-293T) and normalised for input IFNλ using a C-terminal "split luciferase" "HiBiT" tag system. Interestingly, using normalised amounts of protein released into the supernatant of transfected cells, we detected different potencies for each IFNλ, consistent with our previous work (17). In general, IFNλ3 had greater antiviral potency than WT IFNλ4 in both human liver- and gut-derived cell lines. WT IFNλ3 induced stronger and more prolonged STAT1 phosphorylation, higher magnitude of ISG induction, and a stronger antiviral effect than WT IFNλ4, which induced a lower and more transient response. The IFNλ4 K154E variant displayed potency that was more similar to IFNλ3 and shows that, at least for one rare variant, human IFNλ4 has the potential to have significant stimulatory effects. Considering the dynamics of the response, we show clear differences between IFNλ3 and IFNλ4 variants antiviral activity over time. These observations are consistent with previous work on IFNλ4 WT kinetics (20). Interestingly, IFNλ3 and IFNλ4 showed differential characteristics by limiting their contact time with target cells, suggestive of different interactions with receptor complexes. This observation requires more detailed biochemical and cell biology analysis, preferably using purified proteins and receptor molecules that would allow measurement of binding affinities, on–off rates, and their effects on receptor trafficking, for the IFNλ family. Such analysis was beyond the scope of our study primarily due to the inherent technical difficulties of preparing significant quantities of soluble, correctly folded IFNλ4.

The interaction between IFNλs and their receptor complexes remains poorly understood, although several crystal structures of IFNλ proteins, with the exception of IFNλ4, in the presence and absence of its heterodimeric receptor complex IFNλR1 and IL10R2 have been solved (24, 25). There is reason to believe that IFNλ4 is likely to interact differently with its receptors based on amino acid sequence alignments (13, 15). IFNλ4 and IFNλ1/2/3 share only ~30% homology, with highest levels found in the IFNλR1-binding "helix F." Aside from helix F, IFNλ4 differs considerably compared to the other IFNλs, including other receptor binding helices, such as helix D that binds IL10R2. To test the contribution of IFNλ4 receptor interactors in and around helices A, D, and F, we constructed chimeras using IFNλ1 as a reporter for antiviral activity into which we inserted predicted receptor binding domains from IFNλ4. These IFNλ1/IFNλ4 chimeric displayed similar kinetic profiles as IFNλ1 and IFNλ3, although differences in production and potency were noted. This suggests that the molecular determinants that regulate binding kinetics may not lie solely in the putative surface-exposed receptor-binding interfaces that we tested. IFNλ4 differs in structural capacity to IFNλ1/3, which may not be captured in our chimeras, and further differences are observed in other helices that may play roles in signalling. A possible explanation for these differences could be due to differing

stabilities for each of the IFNλs. The stability of each IFNλ has not yet been tested but could provide insight into how each family member achieves its maximal activity. However, as most of our assays were performed in relatively short time frames (2–6 h), it seems unlikely that IFN stability played a role in the differences we observed and is more likely that IFNλ4 interacts and activates the receptor more rapidly, likely through binding more strongly analogous to type I IFNs (23).

An important aspect of our work is that the differences we detected between IFNλ3 and IFNλ4 in antiviral kinetics were conserved in non-human species, through analysis of chimpanzee and macaque IFNλ4 and macaque IFNλ3 in human and macaque cell lines. This is important because compared to other primates, humans appear to have evolved unique IFNλ4 features relevant for outcome of infectious diseases like HCV (13, 14, 17). This finding would be consistent with the limited genetic differences between these species (>90% similarity). The fact that the kinetics are not unique to humans supports the hypothesis that alterations in IFNλ4 potency has been the dominant phenotype that our recent evolution has acted upon. It would be of interest to test further related IFNλ4, from distantly related mammals (22).

Testing IFNλ kinetics in two cell lines allows us to assess conserved and divergent activities in hepatocytes and intestinal cells. IFNλs can signal in many tissues (8), including the human gut (21), and recent work has implicated variants in IFNλ4 in the outcome of enterovirus infection in the respiratory tract but which can infect the gut as well (16). The role of IFNλ4 in intestinal cells up until now has been largely unexplored. Whilst IFNλ3 and IFNλ4 can signal in both cell types, we show clear differences in potency of human IFNλ4 variants, consistent with our previous work in hepatocytes. Comparing the induction of IFNλ signalling in HepaRG and T84 cells suggested that the hepatocyte cell line was more sensitive to IFNλs, yet to draw any conclusions, primary liver and intestinal cells or organoids from several individuals should be tested. Nevertheless, we observed consistent kinetics differences of IFNλ4 compared to IFNλ3 in both cell lines.

Our work has several implications, most importantly those relating to the conserved differences between IFNλ3 and IFNλ4. Compared to type I IFNs, IFNλs have been defined partially by their slower, sustained signalling kinetics (10, 11). IFNλ4 has several unique features, including its association with certain diseases, transcriptional suppression, and evolution in humans, which suggests a degree of specialisation. Unlike other IFNλs, IFNλ4 appears to signal more like type I IFNs despite utilising IFNλR1 and IL10R2. Thus, IFN kinetics may not solely lie in receptor biology but in the interactions between cytokine and receptor. We hypothesise that one outcome of the kinetics of IFNλ1-3 outlined here, where activity is dependent on time and local concentration, would be a more tunable strategy, which may have "adaptive" potential for mucosal surfaces where more robust IFN activities may have pathogenic effects. Whether the unique kinetics of IFNλ4 would provide additional non-redundant therapeutic benefit over other IFNλs remains to be explored.

In conclusion, we provide further evidence of the functional divergence of IFNλ4 compared to other IFNλ proteins supporting the continued investigation into the causes and consequences of such distinctive signalling on the human immune system, which may be exploited for therapeutic gain.

MATERIALS AND METHODS

Cell Lines

HEK-293T (human embryonic kidney) and LLC-MK2 (rhesus macaque respiratory epithelial cell line) were cultured in high glucose Dulbecco's modified Eagle's medium (DMEM) with 10% foetal calf serum (FCS) and pen/strep. HepaRG.ISG15-EGFP [human hepatocyte-like cell line modified to express EGFP under the control of the endogenous ISG15 promoter (17)] were cultured in complete William's media with FCS (10%), human insulin (4 μg/ml), hydrocortisone hemisuccinate (50 μM), and pen/strep (1%) (HepaRG cells). T84 (ATCC CCL-248) colon carcinoma cells were cultured in a 50:50 mix of DMEM:F12 with 10% FCS and 1% pen/strep on collagen-coated cell culture dishes. All cell lines were passaged routinely following PBS washing and trypsin-mediated detachment. Cell lines were routinely screened for *Mycoplasma* contamination and discarded if signs of contamination were detected.

Viruses

Two viruses were used in this study: Ruckart strain of encephalomyocarditis virus (EMCV) and VSV. EMCV was produced in Vero cells following low MOI infection (MOI = 0.0001) and harvested between 1 and 2 days when extensive cytopathic effect was observed. EMCV infectivity was quantified by $TCID_{50}$ and typically grew to titres of ~10^8/ml. VSV-luc was a kind gift from Sean Whelan (Washington University, St. Louis) and was produced and titrated as described in (26, 27).

Antibodies and Reagents

Commercially available primary antibodies were mouse monoclonal antibodies recognizing β-actin (Sigma #A5441), pSTAT1 (BD Transductions #612233), mouse anti-STAT1 antibody (3987, Abcam), or mouse anti-phospho-STAT1 antibody (29025, Abcam) and used at a 1:1,000 dilution. Additionally, rabbit anti-beta-tubulin antibody (6046, Abcam) was also used (1:1,000). For secondary antibodies, antimouse (GE Healthcare #NA934V), coupled with horseradish peroxidase (HRP), was used at a 1:5,000 dilution (T84) or horseradish peroxidase-conjugated goat antirabbit IgG secondary antibody (A0545, Sigma-Aldrich) at 1:2,000 dilution or horseradish peroxidase-conjugated goat anti-mouse IgG secondary antibody (A4416, Sigma-Aldrich) at 1:2,000 (HepaRG).

Molecular Biology

Recombinant DNA technology was utilised to generate the IFNs for functional testing in this study, as previously described (15, 17). The mammalian expression plasmids expressing HiBiT variants and human IFNλ3, and chimpanzee (*Pan troglodytes*)

and rhesus macaque (*Macaca mulatta*) IFNλ4 with a carboxy-terminal FLAG tag were described previously (17). Rhesus macaque IFNλ3-FLAG was generated synthetically (GeneArt) with sequence corresponding to XP_001086865.3 alongside WT IFNλ1-HiBiT, or IFNλ1/λ4-HiBiT chimeras were constructed synthetically (GeneArt) with sequences from helices A, D, and F as shown (**Figure 5**) and cloned into expression vector pC1 and sequenced confirmed by Sanger sequencing. Correct plasmids were purified by midiprep or maxiprep and quality and quantity determined by NanoDrop prior to transfection. An EGFP expression plasmid prepared in identical conditions was used as a negative control throughout.

IFN Production

IFNλs were produced using the protocol described previously, which is capable of generating functional IFNλs (17). Briefly, IFN expression plasmids were transfected into sub-confluent HEK-293T cell monolayers, which are hyporesponsive to IFNλ signalling due to very low expression of IFNλR1 (15). Lipofectamine 2000 was used to transfect IFNλ plasmids per manufacturer's instructions. IFNλs were routinely generated in six-well plates or 10 cm dishes, and 2 and 14 μg of plasmids were used, respectively. Lipofectamine 2000 (2 μl) was used per microgram of plasmid. Plasmids were transfected into cells in Optimem for 16–18 hours, before changing media to growth media (10% FCS) until 2 days posttransfection was reached. The conditioned media were harvested, clarified by centrifugation, aliquoted, and immediately frozen at −80 in. Relative levels of IFNλs were estimated using the extracellular HiBiT split luciferase assay by virtue of their C-terminal HiBiT tag by incubating IFN preparations with assay reagents and measured by manufacturer's instructions (Nano-Glo HiBiT Extracellular Detection system, Promega) using a luminometer.

Interferon Treatments

For quantitative real-time PCR (qRT-PCR) or immunoblotting experiments, IFN stimulation was achieved by incubating cell monolayers with IFNλ-containing conditioned media at a defined concentration to have equivalent HiBiT signal for each sample. Cells treated with IFNs were incubated for the indicated period of time before either being processed. A previous titration analysis indicated that a ~1:2–1:4 dilution of IFNλ4-WT is enough to give a robust induction of ISGs for all variants (17) and antiviral response whilst limiting the amount of conditioned media added to cells (<50% of total volume). Therefore, WT IFNλ4 was used at the standard, and the levels of other IFNs were normalised to this by virtue of the HiBiT tag. Based on HiBiT assay measurements, the relative ratios of supernatant were IFNλ4(WT):P70S:L79F:K154E:IFNλ3, ~1:2:2:0.2:0.01. For the analysis of pSTAT1 levels by immunoblotting, 100,000 cells were seeded in 500 μl of growth media, into sterile rat-tail-collagen-coated (T84) or untreated (HepaRG) 24-well plates. To analyse ISG expression levels by qRT-PCR, 50,000 T84 cells were seeded in 500 μl DMEM/F12 into sterile rat-tail-collagen-coated 48-well plates, or 1,000,000 HepaRG cells were seeded into 2 ml of growth media into 6-well plates. Cells were treated either with HEK293T cell supernatants containing either IFNλ3 or different IFNλ4 variants [λ4 wild type (WT), K154E, P70S] or GFP-conditioned medium (Mock). Prior to treatment, media were removed; cells were rinsed once in PBS and then treated with each IFN diluted in their corresponding growth media to achieve an equal concentration (as determined by HiBiT) and added to the cells in 500–1,000 μl/well. Cells were then incubated at 37°C and 5% CO_2 until harvest. Cells were harvested at 15 min, 30 min, 1 h, 2 h, 4 h, 24 h, and 48 h posttreatment for the analysis of pSTAT1 protein levels by immunoblotting, whereas total RNA was isolated from T84 cells at 2, 4, 8, 12, and 24 h posttreatment for the analysis of ISG expression levels by qRT-PCR. To control for batch-to-batch variability in protein production, at least two independent protein preps were used.

Viral Infections

For the EMCV antiviral assays, 5,000 cells were seeded per well in a 96-well plate 24 h prior to treatment. At the day of treatment, IFNs were added in twofold serial dilutions to the cells 24 h prior to infection. Following IFN treatment, EMCV (MOI = 0.3) was added to the cells, and infection was scored by CPE 24hpi visually or by crystal violet staining. EMCV is highly cytopathic in certain cell lines and very sensitive to IFN. The reciprocal of the dilution giving ~50% protection was used as a semiquantitative measure of IFNλ-conditioned media activity.

For VSV infection, T84 or HepaRG cells were seeded in a white bottom 96-well plate. Cells were pretreated prior to infection as indicated time points and concentrations of IFN-λ3 and IFN-λ4, and its variants K154E and P70S. VSV-luc (MOI = 1) was added to the wells, and the infection was allowed to proceed for 8 h. At the end and the infection, media was removed, cells were washed 1× with PBS and lysed with cell lysis buffer (Promega) at room temperature (RT) for 20 min. The same volume of Steady Glo (Promega) was added to the cells and incubated for 15 min. Luminescence was read using Tecan Infinite M200 Pro.

Immunoblotting

At the time of harvest, cells were rinsed once with PBS and then lysed with 1× radioimmunoprecipitation assay (RIPA) buffer [150 mM sodium chloride, 1.0% Triton X-100, 0.5% sodium deoxycholate, 0.1% sodium dodecyl sulphate (SDS), 50 mM Tris at pH 8.0 supplemented with phosphatase and protease inhibitors (Sigma-Aldrich or Thermo Fisher) for 5–10 min at RT (T84) or ice (HepaRG)]. Cell lysates were collected, and roughly equal amounts of protein were then separated by SDS-PAGE in a 10% (HepaRG) or 12% (T84) polyacrylamide gel, following boiling and reducing. Lysates were then blotted onto a nitrocellulose membrane (T84) or PVDF (HepaRG) by wet blotting. Membranes were blocked with blocking buffer [5% BSA in TBS containing 0.1% Tween-20 (TBS-T)] for 1 h at RT whilst shaking. Primary antibodies (1:1,000 dilution) were diluted in blocking buffer and incubated overnight shaking at 4°C. The membranes were washed four times in TBS-T for 10 min at RT. Then, secondary antibodies were diluted in blocking buffer and incubated for 1 h shaking at RT. Membranes were again washed four times in TBS-T for 10 min at RT. HRP detection reagent (GE Healthcare) was mixed 1:1 and incubated

at RT for 2–3 min, or ECL substrate is added (Immobilon crescendo western HRP substrate, WBLUR0100, Merck). Membranes were then exposed to film and developed or visualised by chemiluminescence using the G:BOX Chemi gel doc Imaging System Instrument (Syngene). The detection of β-actin (T84) or β-tubulin (HepaRG) was used as loading controls. For quantitative analysis, pSTAT1 intensities of each immunoblot were quantified for each timepoint using ImageJ or Image Studio Lite Version 5.2. For quantification with ImageJ, the background value (Mock) was manually subtracted from the calculated values. pSTAT1 levels were then determined relative to control.

RT-qPCR

The total RNA was purified from lysed cells using the Nucleo Spin® RNA extraction kit (T84) by Marchery-Nagel (Catalog number 740955.50) according to the manufacturer's instructions or (HepaRG) RNeasy Mini Kit (74106, Qiagen). RNA concentration was measured using the NanoDrop Lite spectrophotometer (Thermo Scientific). For T84 cells, 250 ng of total RNA was reverse transcribed into cDNA using the iScript™ cDNA Synthesis kit (BioRad Laboratories, Catalog number 1708891). The reaction contained a mixture of 1 µl Reverse Transcriptase, 4 µl Reaction Mix, and 15 µl of RNA template in nuclease-free water. The newly synthesised cDNA was diluted 1:2 in RNase/DNase free water. The following qRT-PCR was performed using a Bio-Rad CFX96 Real-Time PCR Detection System. Per reaction 7.5 µl of SsoAdvanced Universal SYBR Green Supermix, 2 µl of 1:2 diluted cDNA, 1.7 µl of nuclease free water, and 1.9 µl of either forward or reverse primers (2 µM) for the amplification of IFIT1 (fw: 5′-AAAAG CCCACATTTGAGGTG-3′; rev: 5′-GAAATTCCTGAAA CCGACCA-3′), ISG15 (fw: 5′-CCTCTGAGCATCCTGGT-3′; rev: 5′-AGGCCGTACTCCCCCAG-3′), Viperin (fw: 5′-GAGAGCCATTTCTTCAAGACC-3′ and rev: 5′-CTATAATC CCTACACCACCTCC-3′), and Mx1 (fw: 5′-GGTCTATACCACACGCACAGA-3′; rev: 5′- ACTGGTT TCCTTTGCCTCGT-3′) were used. Data analysis was performed using the Bio-Rad CFX Manager 3.0. The expression of the targeted genes was then normalised to the housekeeping gene HPRT1 (fw: 5′-CCTGGCGTC GTGATTAGTGAT-3′; rev: 5′-AGACGTTCAGTCCTGT CCATAA-3′). For HepaRG cells, 1 µg of total RNA was reverse transcribed into cDNA using the High-Capacity cDNA Reverse Transcription Kit (Applied Biosystems, UK). The reaction contained a mixture of 1 µl Reverse Transcriptase, 9 µl Reaction Mix, and 10 µl of RNA template in nuclease-free water. The newly synthesised cDNA was diluted 1:25 in RNase/DNase free water. The following qRT-PCR was performed using a Real-Time Ready PCR Kit (Roche) and TaqMan primer–primer–probe mixes. Each reaction mixture consisted of 10 µl of 2× LightCycler 480 Probes Master, 1 µl of 20× Real-Time Ready Assay with 4 µl PCR-grade H$_2$O (total volume, 15 µl). Template DNA, defrosted on ice, was first diluted 1:25 (v/v) with PCR-grade H$_2$O and then 5 µl diluted template added per reaction tube to the probes MasterMix to give a final volume of 20 µl. TaqMan assays (Catalogue number 4331182) for *IFIT1*

(Assay ID: Hs03027069_s1), *ISG15* (Assay ID: Hs01921425_s1), *MX1* (Assay ID: Hs00895608_m1), and *RSAD2/VIPERIN* (Assay ID: Hs00369813_m1) were used. The expression of the targeted genes was then normalised to the housekeeping gene *GAPDH* (Assay ID: Hs02786624_g1). Cells treated with conditioned media from EGFP-plasmid transfected HEK-293T cells were used as a mock control, and all values were normalised against this value at each time as "fold change to EGFP."

SUPPLEMENTARY MATERIAL

The Supplementary Material for this article can be found online at: https://www.frontiersin.org/articles/10.3389/fimmu.2021. 772588/full#supplementary-material

Supplementary Figure 1 | pSTAT1 quantification over time for IFNλs on liver and gut cells. Quantification of pSTAT1 from images in **Figure 1** compared to house-keeping control and background levels was carried out by densitometry analysis for

HepaRG (A) and T84 (B) cells (IFNλ3-HiBiT [red], IFNλ4-HiBiT: WT [blue], P70S [purple], and K154E [cyan]).

Supplementary Figure 2 | Effect of IFN incubation time on kinetics of human IFNλ variants. HepaRG cells were stimulated with IFNλs: IFNλ3-HiBiT (red), IFNλ4-HiBiT variants: WT (blue), P70S (purple), and K154E (cyan) at indicated times (2, 6 or 24h) before supernatant was removed and rinsed with PBS before being replaced with fresh media not containing virus (A). Stimulated cells were incubated until 24h after IFNλ incubation prior to infection with EMCV and antiviral activity was read 24hpi (B). Error bars represent the mean ± SEM from 2 biological replicates.

REFERENCES

1. Abbafati C, Abbas KM, Abbasi-Kangevari M, Abd-Allah F, Abdelalim A, Abdollahi M, et al. Global Burden of 369 Diseases and Injuries in 204 Countries and Territories, 1990–2019: A Systematic Analysis for the Global Burden of Disease Study 2019. *Lancet* (2020) 396(10258):1204–22. doi: 10.1016/S0140-6736(20)30925-9

2. Heim HM. 25 Years of Interferon-Based Treatment of Chronic Hepatitis C: An Epoch Coming to an End. *Nat Rev Immunol* (2013) 13(7):535–42. doi: 10.1038/NRI3463

3. Bowie AG, Unterholzner L. Viral Evasion and Subversion of Pattern-Recognition Receptor Signalling. *Nat Rev Immunol* (2008) 8(12):911–22. doi: 10.1038/nri2436

4. Isaacs A, Lindenmann J. Virus Interference. I. The Interferon. *Proc R Soc Lond B Biol Sci* (1957) 147(927):258–67. doi: 10.1098/rspb.1957.0048

5. Hoffmann HH, Schneider WM, Rice CM. Interferons and Viruses: An Evolutionary Arms Race of Molecular Interactions. *Trends Immunol* (2015) 36(3):124–38. doi: 10.1016/J.IT.2015.01.004

6. Kotenko SV, Gallagher G, Baurin VV, Lewis-Antes A, Shen M, Shah NK, et al. IFN-Λs Mediate Antiviral Protection Through a Distinct Class II Cytokine Receptor Complex. *Nat Immunol* (2003) 4(1):69–77. doi: 10.1038/ni875

7. Santer DM, Minty GES, Golec DP, Lu J, May J, Namdar A, et al. Differential Expression of Interferon-Lambda Receptor 1 Splice Variants Determines the Magnitude of the Antiviral Response Induced by Interferon-Lambda 3 in Human Immune Cells. *PloS Pathog* (2020) 16(4):e1008515. doi: 10.1371/JOURNAL.PPAT.1008515

8. Sommereyns C, Paul S, Staeheli P, Michiels T. IFN-Lambda (IFN-Lambda) Is Expressed in a Tissue-Dependent Fashion and Primarily Acts on Epithelial Cells in Vivo. *PloS Pathog* (2008) 4(3):e1000017. doi: 10.1371/journal.ppat.1000017

9. Sheppard P, Kindsvogel W, Xu W, Henderson K, Schlutsmeyer S, Theodore E, et al. IL-28, IL-29 and Their Class II Cytokine Receptor IL-28r. *Nat Immunol* (2003) 4(1):63–8. doi: 10.1038/ni873

10. Marcello T, Grakoui A, Barba–Spaeth G, Machlin ES, Kotenko SV, Macdonald MR, et al. Interferons α and λ Inhibit Hepatitis C Virus Replication With Distinct Signal Transduction and Gene Regulation Kinetics. *Gastroenterology* (2006) 131(6):1887–98. doi: 10.1053/j.gastro.2006.09.052

11. Pervolaraki K, Talemi SR, Albrecht D, Bormann F, Bamford CGG, Mendoza JL, et al. Differential Induction of Interferon Stimulated Genes Between Type I Andtype III Interferons Is Independent of Interferon Receptor Abundance. *PloS Pathog* (2018) 14(11):e1007420. doi: 10.1371/journal.ppat.1007420

12. Forero A, Ozarkar S, Li H, Lee CH, Hemann EA, Nadjsombati MS, et al. Differential Activation of the Transcription Factor IRF1 Underlies the Distinct Immune Responses Elicited by Type I and Type III Interferons. *Immunity* (2019) 51(3):451–64.e6. doi: 10.1016/J.IMMUNI.2019.07.007

13. Prokunina-Olsson L, Muchmore B, Tang W, Pfeiffer RM, Park H, Dickensheets H, et al. A Variant Upstream of IFNL3 (IL28B) Creating a New Interferon Gene IFNL4 Is Associated With Impaired Clearance of Hepatitis C Virus. *Nat Genet* (2013) 45(2):164–71. doi: 10.1038/ng.2521

14. Terczyńska-Dyla E, Bibert S, Duong FHT, Krol I, Jørgensen S, Collinet E, et al. Reduced Ifnλ4 Activity Is Associated With Improved HCV Clearance and Reduced Expression of Interferon-Stimulated Genes. *Nat Commun* (2014) 5:5699. doi: 10.1038/ncomms6699

15. Hamming OJ, Terczyńska-Dyla E, Vieyres G, Dijkman R, Jørgensen SE, Akhtar H, et al. Interferon Lambda 4 Signals via the Ifnλ Receptor to Regulate Antiviral Activity Against HCV and Coronaviruses. *EMBO J* (2013) 32(23):3055–65. doi: 10.1038/emboj.2013.232

16. Rugwizangoga B, Andersson ME, Kabayiza JC, Nilsson MS, Ármannsdóttir B, Aurelius JC, et al. IFNL4 Genotypes Predict Clearance of RNA Viruses in Rwandan Children With Upper Respiratory Tract Infections. *Front Cell Infect Microbiol* (2019) 9:340. doi: 10.3389/fcimb.2019.00340

17. Bamford CGG, Aranday-Cortes E, Filipe IC, Sukumar S, Mair D, Flipie ADS, et al. A Polymorphic Residue That Attenuates the Antiviral Potential of Interferon Lambda 4 in Hominid Lineages. *PloS Pathog* (2018) 14(10): e1007307. doi: 10.1371/journal.ppat.1007307. Edited by Glenn Randall.

18. Hong M, Schwerk J, Lim CL, Kell A, Jarret A, Pangallo J, et al. Interferon Lambda 4 Expression Is Suppressed by the Host During Viral Infection. *J Exp Med* (2016) 213(12):2539–52. doi: 10.1084/jem.20160437

19. Zhou H, Møhlenberg M, Terczyńska-Dyla E, Winther KG, Hansen NH, Vad-Nielsen J, et al. The IFNL4 Gene Is a Noncanonical Interferon Gene With a Unique But Evolutionarily Conserved Regulation. *J Virol* (2020) 94(5): e01535–19. doi: 10.1128/JVI.01535-19

20. Obajemu AA, Rao N, Dilley KA, Vargas JM, Sheikh F, Donnelly RP, et al. IFN-λ4 Attenuates Antiviral Responses by Enhancing Negative Regulation of IFN Signaling. *J Immunol* (2017) 199(11):3808–20. doi: 10.4049/jimmunol.1700807

21. Pervolaraki K, Stanifer ML, Münchau S, Renn LA, Albrecht D, Kurzhals S, et al. Type I and Type III Interferons Display Different Dependency on Mitogen-Activated Protein Kinases to Mount an Antiviral State in the Human Gut. *Front Immunol* (2017) 8:459. doi: 10.3389/FIMMU.2017.00459

22. Paquin A, Onabajo OO, Tang W, Prokunina-Olsson L. Comparative Functional Analysis of 12 Mammalian IFN-λ4 Orthologs. *J Interferon Cytokine Res* (2016) 36(1):30–6. doi: 10.1089/jir.2015.0096

23. Schreiber G. The Molecular Basis for Differential Type I Interferon Signaling. *J Biol Chem* (2017) 292(18):7285–94. doi: 10.1074/JBC.R116.774562

24. Gad HH, Dellgren C, Hamming OJ, Vends S, Paludan SR, Hartmann R. Interferon-λ Is Functionally an Interferon But Structurally Related to the Interleukin-10 Family. *J Biol Chem* (2009) 284(31):20869–75. doi: 10.1074/jbc.M109.002923

25. Mendoza JL, Schneider WM, Hoffmann HH, Vercauteren K, Jude KM, Xiong A, et al. The IFN-λ-IFN-Λr1-IL-10rβ Complex Reveals Structural Features Underlying Type III IFN Functional Plasticity. *Immunity* (2017) 46(3):379–92. doi: 10.1016/j.immuni.2017.02.017

26. Cureton DK, Massol RH, Saffarian S, Kirchhausen TL, Whelan SP. Vesicular Stomatitis Virus Enters Cells Through Vesicles Incompletely Coated With Clathrin That Depend Upon Actin for Internalization. *PloS Pathog* (2009) 5 (4):e1000394. doi: 10.1371/JOURNAL.PPAT.1000394

27. Stanifer ML, Cureton DK, Whelan SP. A Recombinant Vesicular Stomatitis Virus Bearing a Lethal Mutation in the Glycoprotein Gene Uncovers a Second Site Suppressor That Restores Fusion. *J Virol* (2011) 85(16):8105–15. doi: 10.1128/JVI.00735-11